Application of a multilaminate model to simulate the undrained response of structured clay to shield tunnelling

H. Kien Dang and Mohamed A. Meguid

Abstract: A constitutive model based on the multilaminate framework has been implemented into a finite element program to investigate the effect of soil structure on the ground response to tunnelling. The model takes into account the elastic unloading–reloading, inherent and induced anisotropy, destructuration, and bonding effects. The model is successfully calibrated and used to investigate the undrained response of structured sensitive clay in the construction of the Gatineau tunnel in Gatineau, Quebec. Numerical results were compared to the field measurements taken during tunnel construction. To improve the performance of the numerical model, an implicit integration algorithm is implemented and proven to be very effective when coupled with the multilaminate framework as compared to the conventional explicit integration methods. The effect of different soil parameters including bonding and anisotropy on the tunnelling induced displacements and lining stresses is also examined using a comprehensive parametric study. The results indicated that soil bonding and anisotropy have significant effects on the shape of the settlement trough as well as the magnitudes of surface displacements and lining stresses induced by tunnelling.

Key words: constitutive modelling, soil–structure interaction, tunnelling, finite element, multilaminate model.

Résumé : Un modèle constitutif basé sur un cadre multilaminé a été mis en application dans un programme d'éléments finis pour étudier l'effet de la structure du sol sur la réponse du terrain lors du creusage de tunnel. Le modèle prend en compte le chargement et déchargement élastiques, l'anisotropie inhérente et induite, les effets de la déstructuration et de la formation de liens. Le modèle est successivement calibré et utilisé pour étudier la réponse non drainée de l'argile sensible structurée lors de la construction du tunnel Gatineau, à Gatineau, Québec. Les résultats numériques ont été comparés aux mesures sur le terrain prises durant la construction du tunnel. Pour améliorer la performance du modèle numérique, un algorithme d'intégration implicite est mis en application et on a prouvé qu'il était très efficace lorsque couplé avec le cadre multilaminé en comparaison avec les méthodes d'intégration explicites conventionnelles. Au moyen d'une étude paramétrique complète, on examine aussi l'effet de différents paramètres du sol incluant les liens et l'anisotropie sur les déplacements et les contraintes dans la garniture induits par le creusage de tunnels. Les résultats indiquent que les liens et l'anisotropie du sol ont des effets appréciables sur la forme du creux de tassement de même que sur les amplitudes des déplacements de surface et sur les contraintes dans la garniture induites par le creusage du tunnel.

Mots-clés : modélisation constitutive, interaction sol–structure, creusage de tunnel, éléments finis, modèle multilaminé.

[Traduit par la Rédaction]

Introduction

Ground response to tunnelling has been conventionally analyzed based on closed form solutions (e.g., Peck 1969; Sagaseta 1987; Verruijt and Booker 1996; Loganathan and Poulos 1998; and Park 2004), semi-analytical solutions (e.g., Rowe 1983 and Lo et al. 1984), or numerical solutions (e.g., Lee and Rowe 1990*a*, 1990*b*; Addenbrooke et al. 1997; and Potts and Addenbrooke 1997). The numerical methods provide the flexibility of simulating different tunnel geometry and excavation sequence, and allow for the application of advanced soil models. It has been recognized by geotechnical engineers and researchers that constitutive models that account for all of the known characteristics of soil behaviour (e.g., strength anisotropy, rotation of principal stresses, bonding effects, viscous effects, etc.) are difficult to use, and a relevant model is usually employed to solve a given practical geotechnical problem. Among these soil characteristics, the strength anisotropy and rotation of principal stresses are known to have a significant effect on the modelling of geotechnical problems.

The Critical State model developed at Cambridge (Wood 1990) for normally consolidated and lightly overconsolidated clays is an isotropic hardening model and does not account for the rotation of principal stresses. Anisotropic hardening models (e.g., Wood and Graham 1990; Dafalias et al. 2002) do account for the rotation of principal stresses

Received 15 September 2006. Accepted 3 July 2007. Published on the NRC Research Press Web site at cgj.nrc.ca on 8 February 2008.

H.K. Dang. Department of Civil Engineering and Applied Mechanics, McGill University, 817 Sherbrooke Street West, Montréal, QC H3A 2K6, Canada.
M.A. Meguid.[1] Department of Civil Engineering and Applied Mechanics, McGill University, 817 Sherbrooke Street West, Montréal, QC H3A 2K6, Canada.

[1]Corresponding author (e-mail: mohamed.meguid@mcgill.ca).

 doi:10.1139/T07-066

through a transitional rule described for the yield surface. However, the parameters of these models are based on tests in which no rotation of principal stresses takes place (Pande and Sharma 1983).

Several constitutive models have been developed in the past two decades to capture the specific characteristics of soft clays. Wood and Graham (1990) and Dafalias et al. (2002) modified the well-known Modified Cam Clay (MCC) to account for the anisotropic elasticity and reconstructed the yield loci to match the experimental observations. These models do not account for the strength anisotropy of the clay material. Kumbhojkar and Banerjee (1993) employed the plastic strains as a hardening parameter rather than the volumetric strain; however, the results did not match well with the experimental data. Furthermore, the model is complicated due to the large number of parameters required to define the yield surface. Another model that accounts for the undrained shear strength anisotropy was developed by Su et al. (1998). The model was used to investigate the effect of principal stress orientation on the behaviour of saturated clays. The model parameters required two specific tests, namely, undrained compression after K_o consolidation (CK_oUC) and undrained extension after K_o consolidation (CK_oUE). The suitability of this criterion to model soft clays has been proven to be limited. Sun et al. (2004) modified the anisotropic hardening elastoplastic model for clay, which is also based on the MCC.

Wheeler et al. (2003) presented elastoplastic constitutive model S-Clay1 that accounts for plastic anisotropy by incorporating two hardening rules, the first describes the change of the yield surface size and the second describes the inclination of the yield surface due to the gradual rearrangement of the soil fabric. The results were found to be somewhat scattered from the field measurement.

A multilaminate framework for modelling soft clay has been introduced by Pande and Sharma (1983) based on the work of Calladine (1971). Extensions to the model have been presented by several authors (e.g., Pietruszczak and Pande 2001; Schuller and Schweiger 2002; Wiltafsky et al. 2002; Cudny and Vermeer 2004) to model the inherent anisotropy and destructuration of soft clays.

The objective of this study is to investigate the effect of bonding, anisotropy, and destructuration of clays on the ground movements induced by tunnelling in structured clay using the multilaminate framework. Of course, tunnelling involves three-dimensional stress redistribution in the ground, especially near the tunnel face. For the sake of simplicity, all analysis presented in this study are conducted under plane strain conditions. A brief overview of the multilaminate concept is provided in the following section.

An overview of the multilaminate framework

The concept of multilaminate modelling is based on intersecting a solid block of homogenous, isotropic, elastic material with an infinite number of randomly oriented planes (Pande and Sharma 1983). These planes render the solid block into an assemblage of perfectly fitting polyhedral blocks (Fig. 1), which have rough surfaces behaving in an elastoviscoplastic manner. It is assumed that the overall deformational behaviour of the clay can be obtained by evaluating the deformations along these planes under the current effective normal and shear stresses (σ_n, τ). The opening–closing of the interboundary gap (void ratio) in relation to the initial gap (initial void ratio) is a contributing factor in evaluating deformations. It is also assumed that all contact boundaries have the same characteristics in sliding with no interaction between them.

Since the introduction of the multilaminate framework for the analysis of clayey soils in 1983, several improvements and extensions have been introduced. A multilaminate plasticity formulation was presented by Pietruszczak and Pande (1987) to account for the volumetric and deviatoric hardening of soils. Karstunen and Pande (1997) incorporated the deviatoric hardening and nonassociated flow rule in their multilaminate formulation. The model was used to simulate the shear band formation in NATM tunnelling (Schuller and Schweiger 2002). Wiltafsky et al. (2002) presented a formulation employing the double hardening and volumetric hardening rules. A new version of the multilaminate model was presented by Cudny and Vermeer (2004) to account for the anisotropy and destructuration of soft clay.

Sampling planes

As discussed earlier, the concept of sampling planes is important in the formulation of multilaminate-based constitutive models. Loading imposed on clay blocks results in plastic strains developing along these contact planes. Contribution of plastic strain from all planes is spatially averaged to obtain the plastic increment of the macro strain tensor

$$[1] \qquad \mathrm{d}\varepsilon^p = \sum_{i=1}^{\infty} \mathrm{d}\varepsilon^{pk}$$

In the numerical implementation, this averaging of infinite number of planes is not impossible but it requires a large amount of computation. Therefore, some integration rules are needed. Pietruszczak and Pande (1987) proposed a 13-planes integration rule for 3D analyses and a 9-planes integration rule for plane strain. Due to the development in computer technology, higher order integration rules are feasible today. An integration rule employing 64 contact planes is used by Cudny and Vermeer (2004).

Equation [1] can be calculated using a numerical integration with a chosen scheme of sampling plane. The global plastic strain increment can be written as (Pietruszczak and Pande 1987)

$$[2] \qquad \mathrm{d}\varepsilon^p = \sum_{k=1}^{m} T_{ij}^{\varepsilon k} \mathrm{d}\varepsilon_j^{pk} w_k = \sum_{k=1}^{m} \mathrm{d}\lambda^k T_{ij}^{\varepsilon k} \frac{\partial g^k}{\partial \sigma_j^k} w_k \qquad i = 1, \ldots, 6$$

where w_k is the weight coefficient of the kth plane in integration rule, $\mathrm{d}\lambda^k$ is the plastic multiplier of the kth plane, and g is the potential function on the kth plane.

The transformation matrix from the microplastic strain increment to the global plastic strain increment $T^{\varepsilon\kappa}$ is calculated similar to $T^{\sigma\kappa}$ but based on the transpose matrix D^{kT}

$$[3] \qquad \varepsilon_{ij}^k = D^{k^T} \sigma D^k$$

It is worth noting that $T^{\varepsilon k} = T^{\sigma k^T}$

Fig. 1. Schematic description of the multilaminate framework (adapted from Cudny and Vermeer 2004).

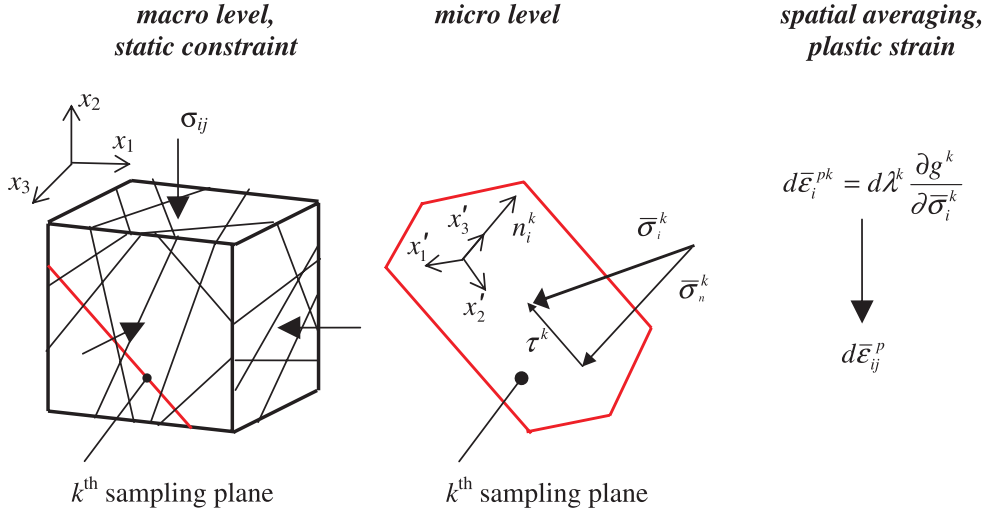

Strength anisotropy

Strength anisotropy of the soil was not accounted for in the early development of the multilaminate framework, (Pande and Sharma 1983, Pande and Yamada 1994). However, stress induced anisotropy was considered by setting the initial anisotropic stress condition (K_o). This means that initial values of preconsolidation stress will be different on every sampling plane. As indicated by Cudny and Vermeer (2004), the degree of anisotropy gained from the initialization of the K_o stress state, in most cases, was found to be too small compared with experimental results.

A formulation that accounts for the soil strength anisotropy was introduced by Pietruszczak and Mroz (2000) by incorporating microstructure tensors. Generally, the directional distribution of the scalar parameter α is obtained using an isotropic value α_0 as follows:

$$[4] \qquad \alpha = \alpha_0(1 + \Omega_{ij} l_i l_j)$$

where l_i, l_j are the units specifying the loading vector and Ω is the deviatoric measure of the material microstructure defined as

$$[5] \qquad \Omega_{ij} = (a_{ij} - \frac{1}{3}\delta_{ij} a_{kk})/(\frac{1}{3} a_{kk})$$

Cudny and Vermeer (2004) indicated that for material like soft clays, it is more reasonable to distribute the overconsolidation ratio directly in relation to the bonding of soil fabric. Consequently, in this study, the mean value of the bonding parameter, x, was varied on each sampling plane.

Model formulation

The fabric anisotropy of clays influences both the elastic and plastic behaviour. Elastic anisotropy has been reported (Graham and Houlsby 1983) to have an impact on the stress path and consequent yielding. However, for the particular application of soft ground tunnelling, studies have shown that elastic anisotropy does not have a significant impact on the induced settlement profile (Addenbrooke et al. 1997; and Franzius et al. 2005). Since tunnelling induced soil movement is of primary interest in this study, isotropic elasticity was therefore adopted.

Another important aspect of tunnelling is the fact that soil in the vicinity of the tunnel may be subjected to cycles of unloading and reloading conditions. This has been considered by modifying the original model of Cudny and Vermeer (2004) to allow the state of stress of each element to be checked during the analysis. The appropriate loading–unloading constitutive relation is employed accordingly. Further details are provided below.

Elastic behaviour

The relationship between stress and strain increments is

$$[6] \qquad \mathrm{d}\sigma_{ij} = D^{\mathrm{e}}_{ijkl} \mathrm{d}\varepsilon^{\mathrm{e}}_{kl}$$

where D^{e} is the elastic stiffness.

The hypoelastic stiffness based on Hooke's law (often used in critical state models) was chosen in the present study for both loading and unloading conditions (Van Baars 2003).

For primary loading

$$[7] \qquad D^{\mathrm{e}}_{ijkl} = \frac{E(p)}{(1+\upsilon)(1-2\upsilon)}[\upsilon\delta_{ij}\delta_{kl} + \frac{1-2\upsilon}{2}(\delta_{ik}\delta_{jl} + \delta_{jk}\delta_{il})]$$

where ν is Poisson's ratio for the loading condition, $E(p)$ is the pressure dependent Young's modulus defined as $E(p)= [3p(1 - 2\upsilon)]/\lambda^*$, and λ^* is the modified compression index estimated from $\ln p$–ε_v diagrams.

For unloading and reloading

$$[8] \qquad D^{\mathrm{e}}_{ijkl} = \frac{E(p)}{(1+\upsilon)(1-2\upsilon)}[\upsilon\delta_{ij}\delta_{kl} + \frac{1-2\upsilon}{2}(\delta_{ik}\delta_{jl} + \delta_{jk}\delta_{il})]$$

where $\nu = \nu_{ur}$ is Poisson's ratio for the unloading and reloading condition, $E(p)$ is the pressure dependent Young's

modulus defined as $E(p)= [3p(1 - 2\upsilon_{ur})]/\kappa^*$, and κ^* is the modified swelling index estimated from $\ln p$–ε_v diagrams.

The unload–reloading parameters are very important in tunnel modelling since the soil around the tunnel being excavated is under unloading condition.

Sampling planes

As mentioned previously, the solution for eq. [1] can be obtained using numerical integration rules. The higher the number of planes, the more accurate the calculated response. In this study, an integration rule with 64 sampling planes is used (see Fig. 2). This integration has been successfully used by other researchers (e.g., Schuller and Schweiger 2002).

Microstructure tensor

To model the structural cross-anisotropy, the microstructure tensor, Ω, is used. One parameter Ω_v, which defines the spatial bias of cross-anisotropic microstructure is needed (Pietruszczak and Mroz 2000)

$$[9] \qquad \Omega_{ij} = \begin{bmatrix} -\Omega_v/2 & 0 & 0 \\ 0 & \Omega_v & 0 \\ 0 & 0 & -\Omega_v/2 \end{bmatrix}$$

Based on eq. [4], the directional attribution can be written as

$$[10] \qquad \alpha = \alpha_0(1 + \Omega_{ij} l_i l_j) = \alpha_0(1 + \Omega_{ij} n_i^k n_j^k) = \alpha_0[1 - \frac{\Omega_v}{2}(n_2^k)^2]$$

where n^k is the unit vector normal to the kth sampling plane.

Yield surface, potential function, and hardening rule

The constitutive model used in this study was based on that reported by Cudny and Vermeer (2004). Model calibration and element tests were also reported in the above reference. A brief description of the model is given below:

As shown in Fig. 3, the micro yield surface consists of two parts: a cone and a cap, which are responsible for shear and compressive strengths, respectively.

The cone part follows Mohr–Coulomb with nonassociated flow rule. The yield and plastic potential functions are defined as

$$[11] \qquad f_{\text{cone}}^k = \tau^k - \sigma_n^k \mu - c$$

$$[12] \qquad g_{\text{cone}}^k = \tau^k - \sigma_n^k \tan\psi$$

Fig. 2. Integration rule over a sphere (adapted from Fliege and Maier 1996).

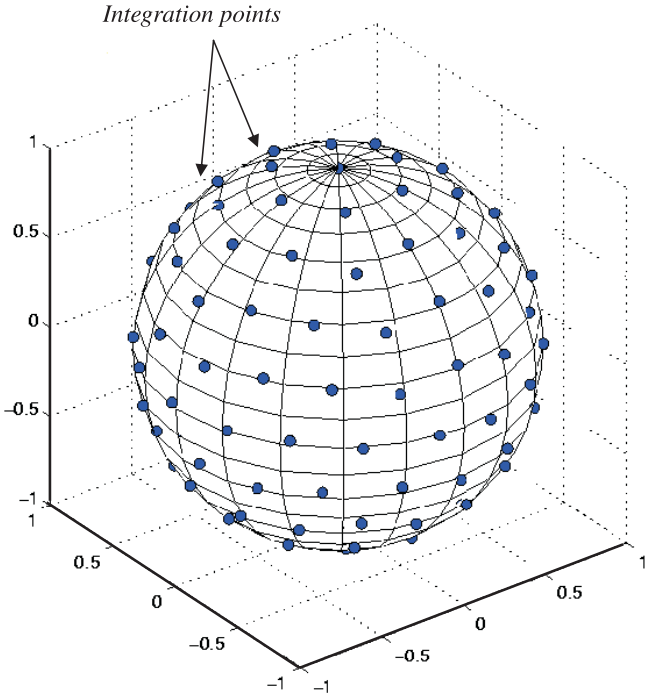

where $\mu = \tan\varphi$ and φ, c, ω are the effective friction angle, effective cohesion, and dilatancy angle, respectively.

The cap part of the yield surface is based on the MCC model and accounts for the bonding affect of natural clays. The yield function of the cap part can be written as

$$[13] \qquad f_{\text{cap}}^k = (\sigma_n^k - \sigma_{np}^k)\mu^2[\frac{2\beta c}{\mu} + (1+\beta)\sigma_n^k + (-1+\beta)\sigma_{np}^k] + (\tau^k\beta)^2(1+\beta) = 0$$

where σ_{np}^k is a micropreconsolidation pressure, and β is an additional parameter that controls the steepness of the cap surface. The later allows the direct model calibration with the asymptotic valued obtained from standard oedometer tests. For $\beta = 1$, the cap surface coincides with the MCC.

The preconsolidation pressure is calculated based on Gens and Nova (1993) as follows:

$$[14] \qquad \sigma_{np}^k = \sigma_{neq}^{0k}(1 + b_0^k), \qquad b_0^k = b_0[1 + \Omega_v(n_2^k)^2]$$

where b_0 is the isotropic or average bonding parameter representing the structural bonding of the clay

$$\sigma_{neq}^{0k} = \frac{\sigma_n^{0k} - \frac{\beta}{\mu}[-c + \sqrt{(c + \sigma_n^{0k}\mu)^2 + (-1+\beta^2)(\tau^{0k})^2}]}{1-\beta}$$

or

$$\sigma_{neq}^{0k} = \sigma_n^{0k} + \frac{(\tau^{0k})^2}{\mu(c + \sigma_n^{0k}\mu)} \qquad \text{for} \quad \beta = 1$$

For the unbounded hardening component, the standard law for normally consolidated clay is employed

$$[15] \qquad \sigma_{np}^{k*} = \sigma_{np}^{0k*} \exp\left(\frac{\varepsilon_n^{pk}}{\lambda* - \kappa*}\right)$$

where ε_n^{pk} is the normal invariant of plastic microstrain and $\lambda*$ and $\kappa*$ are modified compression and swelling indices, respectively, and can be estimated using $\ln p$–ε_v diagrams.

Fig. 3. Yield surface on sampling plane (adapted from Cudny and Vermeer 2004).

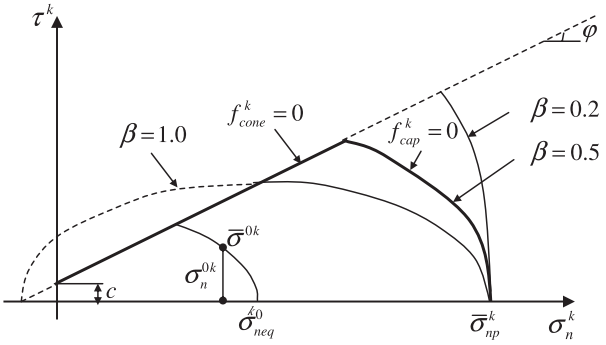

The parameter b^k governs the shrinkage or bonded yield locus and is defined as

$$[16] \qquad b^k = b_0^k \exp\left(-a|\varepsilon_n^{pk}|\right)$$

where a is an additional parameter describing the reduction of bonding with increasing accumulated normal plastic strain $b^k = |\varepsilon_n^{pk}|$

The resultant hardening law for the preconsolidation pressure on the kth sampling plane may be written as

$$[17] \qquad \sigma_{np}^k = \sigma_{np}^{k*}(1 + b^k)$$

The maximum value for parameter a is expressed by

$$[18] \qquad a < a_{max}^k = \frac{1 + b_0^k}{b_0^k(\lambda * - \kappa *)}$$

It was realized (Cudny and Vermeer 2004) that using the minimum value of a_{max}^k for the parameter a may result in a very slow and not realistic destructuration on the planes where a_{max}^k is high. It was found that instead of adopting a as the model parameter, it is better to impose the ratio

$$[19] \qquad a_r = \frac{a^k}{a_{max}^k}$$

Model implementation and calibration

The constitutive model was implemented into PLAXIS finite element program (Plaxis 2004) using the user-defined soil model module. The strain increments are used to calculate the macrostress state. For plane strain conditions, the transformation matrix given below (3×6) was used to transform the macrostresses to microstresses acting on each sampling plane.

$$[20] \qquad T^{\sigma k} = \begin{bmatrix} 0 & 0 & 0 & 0 & -n_2^k & n_1^k \\ -n_1^k n_2^k & n_1^k n_2^k & 0 & -(n_1^k)^2 + (n_2^k)^2 & 0 & 0 \\ (n_1^k)^2 & (n_2^k)^2 & 0 & 2n_1^k n_2^k & 2n_2^k n_3^k & 0 \end{bmatrix}$$

where n^k is a normal vector of the sampling plane.

The microplastic strains on each sampling plane can be calculated using eqs. [11], [12], and [13]. The microplastic strains are assembled into the global plastic strain using eq. [2] to update the macrostresses.

$$[21] \qquad \sigma_i = \sigma_i^0 + D_{ij}^{ek}(\mathrm{d}\varepsilon_j^{ek} - \mathrm{d}\varepsilon_j^{pk})$$

where σ_i, σ_i^0 are previous and current stresses, respectively, and $\mathrm{d}\varepsilon_j^{ek}$ and $\mathrm{d}\varepsilon_j^{pk}$ are input strain increments. The macroplastic strains are calculated using the subroutine incorporated into the finite element program.

Two approaches were used to accelerate convergence; namely, the substep method and the implicit integration scheme. The second has proven to be effective when used in combination with the multilaminate model. Details of the model implementation are given elsewhere (Dang 2006).

The original model was successfully calibrated using element tests under different loading conditions (Cudny and Vermeer 2004). Additional tests were also conducted by Dang (2006). An example of collapse load calculation is discussed below.

A Mohr–Coulomb model associated with the multilaminate framework was first used to calculate the failure load of a strip footing (of unit width) in both undrained and drained conditions assuming weightless soil and constant elastic modulus with depth. The following parameters are used in the analysis:

- Undrained condition: E' = 100 000 kN/m^3, υ' = 0.3, c_u = 10 kPa
- Drained condition: E' = 100 000 kN/m^3, υ' = 0.3, c' = 10 kPa, $\varphi' = 20^\circ$, $\psi = 0$

The resulting soil displacement and failure load for the drained condition were found to be in good agreement with the classical Mohr–Coulomb predictions as shown in Fig. 4. For the undrained condition, the calculated displacement was also found to be in good agreement; however, the failure load calculated using the multilaminate framework was approximately 5% higher, which is considered to be practically acceptable (see Fig. 5).

Effect of the model parameters

The effect of different parameters used in the multilaminate model on the calculated results is examined in this section by incrementally varying each parameter. The following standard and intrinsic soil parameters were used in the analysis:

Standard parameters: $\varphi' = 20^\circ$, c' = 10 kN/m^2, $\psi = 0^\circ$, $\upsilon = \upsilon_{ur} = 0.2$, $\kappa^* = 0.02$, $\lambda^* = 0.1$

Intrinsic parameters: $\beta = 1$, $b_0 = 1$, $\Omega_v = 0.5$, $a_r = 1$

where φ', c', ψ are the effective friction angle, effective cohesion, and dilatancy angle, respectively, β is the parameter controlling the shape of the cap, b_0 is the isotropic or

Fig. 4. Load displacement curve of a strip footing (drain condition).

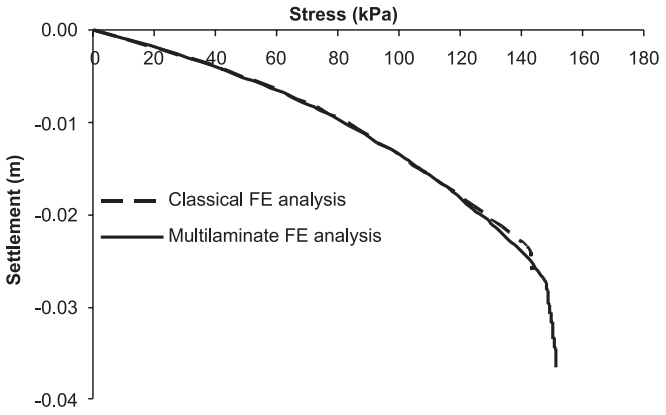

Fig. 5. Load displacement curve of a strip footing (undrained condition).

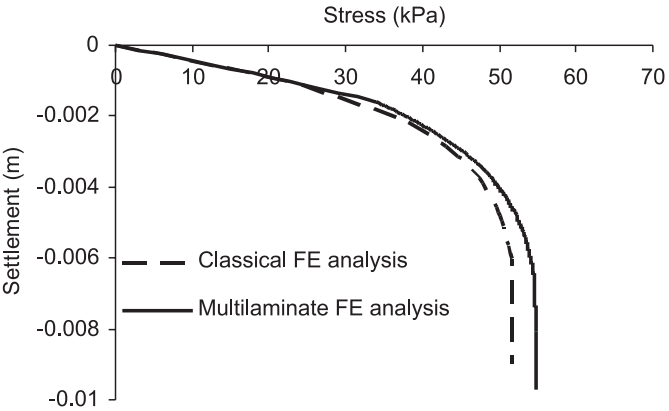

Fig. 6. Influence of the bonding parameter, b_0.

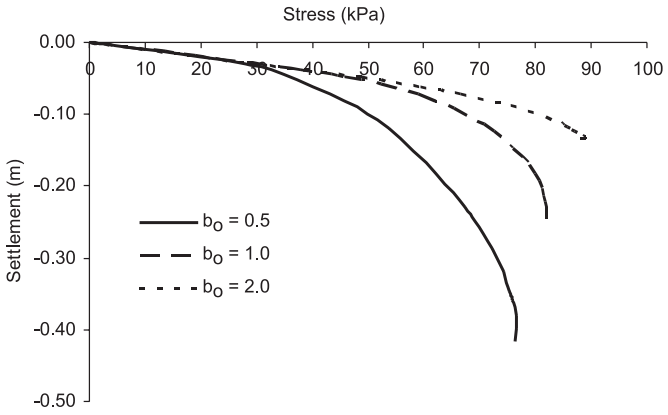

Fig. 7. Influence of the cap parameter, β.

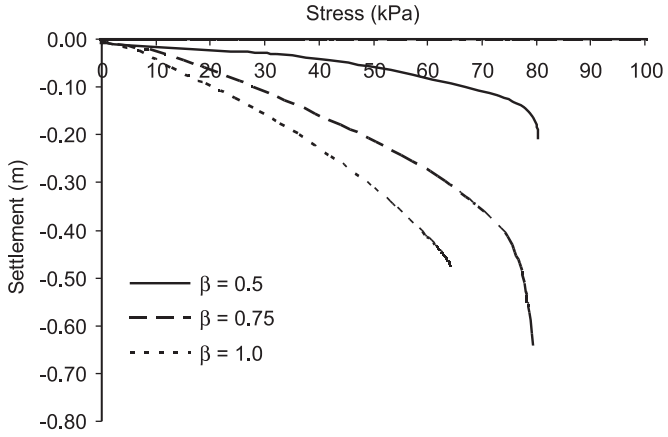

average bonding parameter, and Ω_v is a parameter identifying the spatial bias of cross-anisotropic microstructure.

The bonding parameter, b_0

To examine the effect of the bonding parameter, the value of b_0 was incrementally increased from 0.5 to 2 and the analysis was conducted for each case. It was observed that the bonding parameter has significant effects on the maximum stress and the corresponding displacement at failure as shown in Fig. 6. As b_0 increased from 0.5 to 1, the failure load increased by about 15%, and the displacement decreased by about 50%. With a further increase in the value of b_0, the soil response was found to be stiffer with consistent decrease in displacement.

The cap parameter, β

Figure 7 shows the results for the cases of β = 0.5, 0.75, and 1, which correspond to three different shapes of the cap part of the yield surface (see Fig. 3). It was found that the shape of the cap grew and the soil became stiffer as the value of β decreased from 1 to 0.5. However, the maximum stress at failure did not significantly change for the examined range of β. It should be noted that for β = 1, the analysis was terminated before the failure load was reached due to slow convergence.

Analysis of the Gatineau tunnel

The Gatineau tunnel is located along Champlain Street in the City of Gatineau, Quebec. A key map of the tunnel location is provided in Fig. 8. The tunnel was constructed using a 3.5 m diameter tunnel boring machine (TBM) under a soil cover of approximately 17.5 m below ground surface. This project was chosen because Champlain clays in this area are known to have moderate sensitivity and strong structure (Leroueil et al. 1985). This was evident from the in situ testing results reported in the the geotechnical report by Ballivy et al. (1983). As shown in Fig. 9, the soil along the tunnel alignment consists of a surface layer of dense sand and gravel (standard penetration test (SPT) number of 25) extends to a depth of 2.5 m below ground surface followed by a marine clay layer of approximately 20 m in thickness overlying glacial till overlying bedrock. The clay sensitivity ranges between 2.7 and 6.8. In situ vane shear tests indicated a range of undrained shear strength between 75 and about 190 kPa. Groundwater was found to be located at a depth of about 4 m below ground surface.

Analysis details

The undrained analysis of the Gatineau tunnel construction is conducted using the implemented multilaminate

Fig. 8. Location of the Gatineau tunnel (adapted from Ballivy et al. 1983).

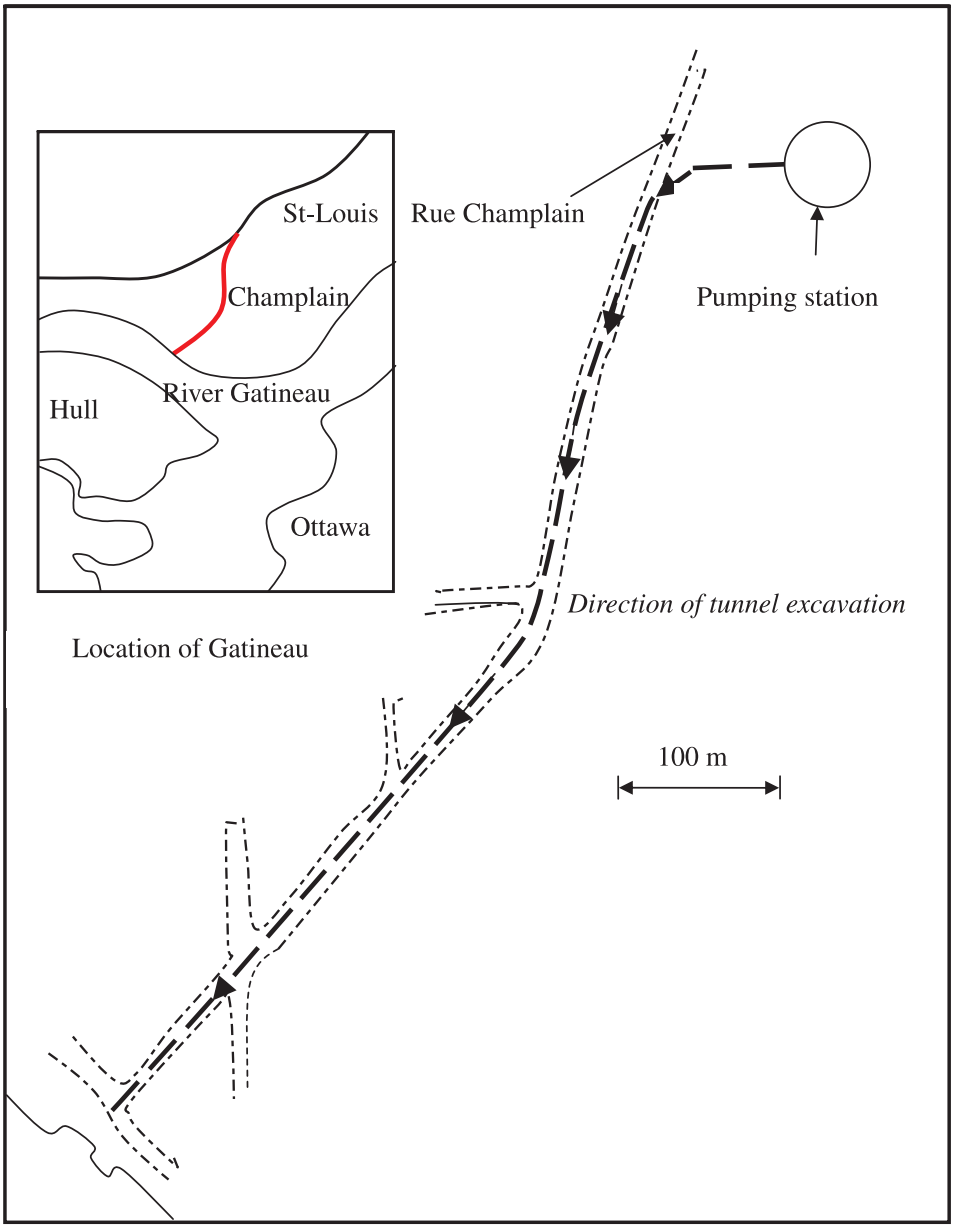

model. The finite element mesh used throughout the analysis is shown in Fig. 10. To capture the undrained shear strength profile of the clay layer, the layer was divided into four sublayers and an average shear strength value was used for each sublayer. Clay parameters required for the multilaminate model were obtained using correlations with the available soil properties as follows:

- The modified compression index was correlated to the soil plasticity index as follows (Plaxis 2004): $\lambda^* = I_p/500$
- The modified swelling index was taken to be about 0.25 of the modified compression index. This is considered to be a reasonable estimate for clays (Leroueil et al. 1985).
- Typical effective friction angle for the Champlain clay ranges from 28° to 31° (Leroueil 1992). A friction angle of 31° was adopted in this study.
- The overconsolidation ratio, OCR, was calculated using the following equation:

$$[22] \qquad \frac{s_u}{\sigma'_{vo}} = 0.2 + 0.0024 I_p$$

where I_p is the plastic index.

- A constant value for the anisotropy parameter, Ω_v, was used for all sublayers. The bonding effect parameter, b_0, is related to the overconsolidation ratio and the anisotropy parameter based on eq. [14] (assuming $OCR_v = \sigma^k_{np}/\sigma^{0k}_n$) as follows:

$$[23] \qquad b_0 = \frac{OCR_v - 1}{1 + \Omega_v}$$

- The coefficient of earth pressure at rest was taken as

Fig. 9. Geotechnical profile (adapted from Ballivy et al. 1983).

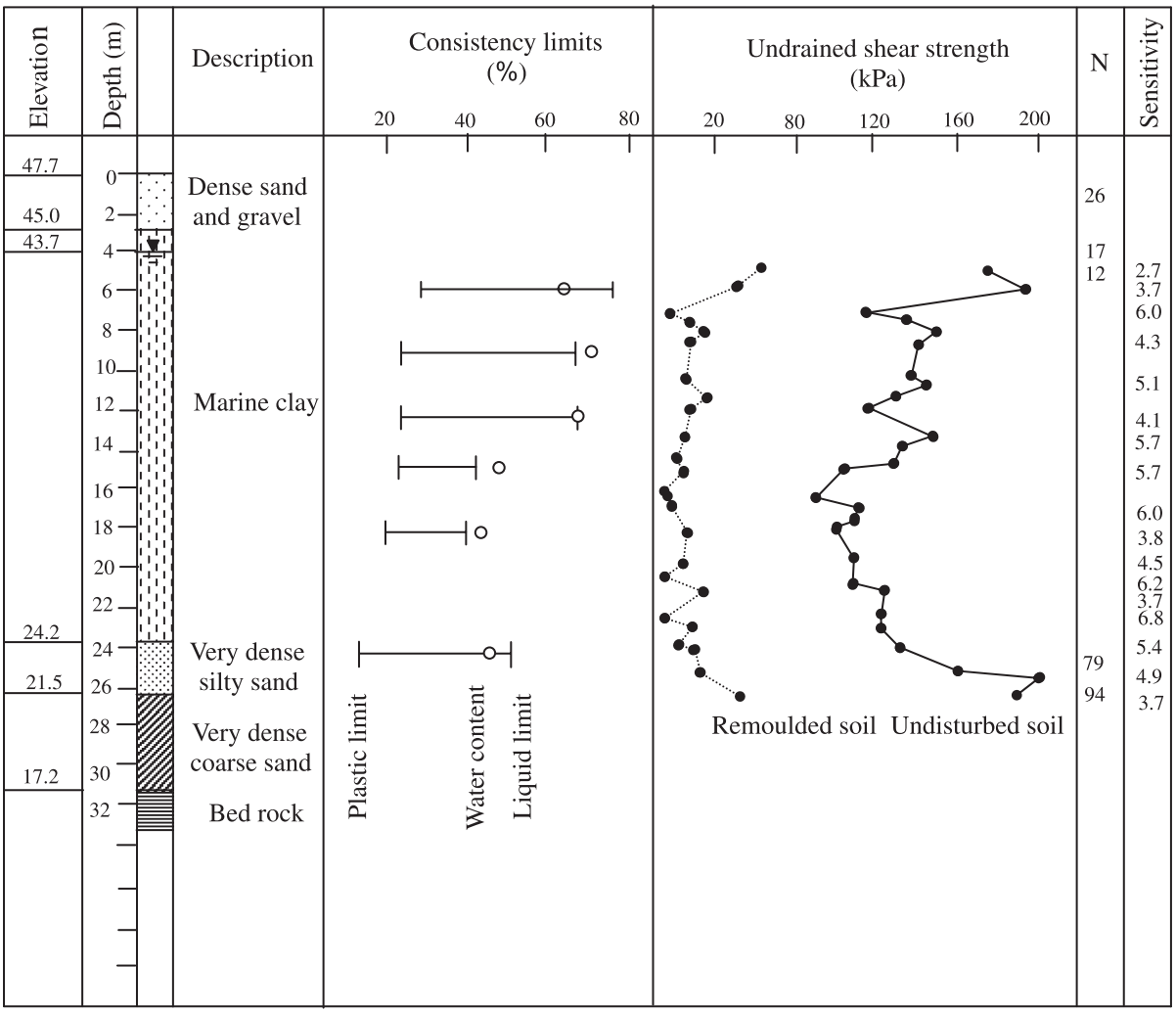

$$[24] \qquad K_o = \mathrm{OCR}^{0.95}$$

The soil properties adopted for each layer are summarized in Table 1. It should be noted that the sand layer (layer No. 1) was modeled using the conventional Mohr–Coulomb failure criterion.

The analysis allowed the calculation of soil displacements around the tunnel and near the ground surface. The results are then compared with the recorded displacements at a given cross section behind the tunnel face.

To investigate the effect of soil structure on the tunnelling induced displacements, the calculated settlement trough for the Gatineau tunnel was compared with the field measurement as well as with the well known Peck's solution (Peck 1969). The shape of the settlement trough is found to be in good agreement with Peck's solution as shown in Fig. 11. A maximum surface settlement of 0.73 cm was calculated above the tunnel centreline near the ground surface, which is in good agreement with the field measurement (0.9 $\pm$ 0.3 cm) taken during the tunnel construction. A radial stress of 92 kPa was calculated at the tunnel crown and is found to reasonably agree with the stress measured (85 kPa) after the tunnel construction.

Parametric study

The effects of soil anisotropy, bonding, OCR, destructuration, and volume loss on the surface settlement and lining stresses for the Gatineau tunnel are examined in the following sections.

Effect of bonding and anisotropy

As discussed in the previous section, for a given value of OCR the bonding parameter, b_0, and the anisotropy parameter, Ω_v, are related by eq. [23]. Based on this relation, the anisotropy parameter, Ω_v, is inversely proportional to the bonding parameter b_0. Therefore, the effect of both parameters is assessed in this parametric study by varying only the anisotropy parameter, Ω_v.

Figure 12 shows the effect of changing the anisotropic parameter, Ω_v, on the shape of the settlement trough. For Ω_v values greater than 2, a negative microstructure tensor is calculated. Therefore, the range of Ω_v was limited to the

Fig. 10. Finite element mesh.

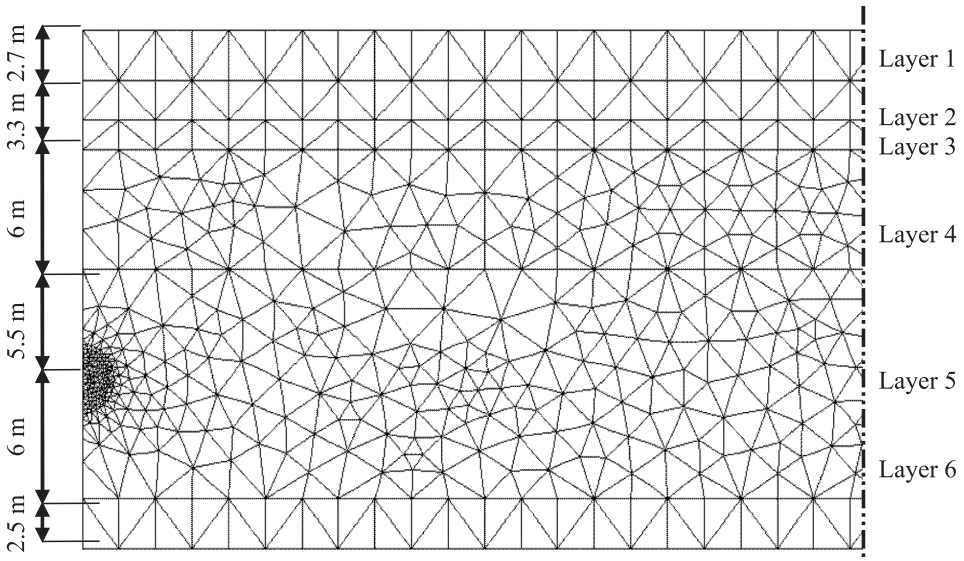

Table 1. Soil properties.

Layer No.	Length (m)	ϕ (°)	c (kPa)	ψ (°)	ν	ν_{re}	λ^*	κ^*	Ω_{ϖ}	a_r	OCR	b_0	K_o
1	2.7	15	0.1	N/A	0.2	N/A	N/A	N/A	N/A	N/A	1.00	N/A	0.74
2	1.3	31	0.1	0	0.3	0.1	0.100	0.025	1.20	1.00	9.65	3.93	1.80
3	2	31	0.1	0	0.3	0.1	0.100	0.025	1.20	1.00	6.51	2.5	1.60
4	6	31	0.1	0	0.3	0.1	0.096	0.025	1.20	1.00	3.25	1.02	1.43
5	12	31	0.1	0	0.3	0.1	0.044	0.011	1.20	1.00	2.09	0.46	1.07
6	2	31	0.1	0	0.3	0.1	0.080	0.020	1.20	1.00	1.96	0.43	1.01

Note: ϕ, effective friction angle; c, effective cohesion; ψ, dilitancy angle; ν, Poisson's ration for the loading condition; ν_{re}, Poisson's ration for the unloading–reloading condition; λ^*, modified compression index; κ^*, modified swelling index; Ω_{ϖ}, deviatoric measure of the material microstructure; a_r, an additional parameter describing the reduction of bonding; OCR, overconsolidation ratio; b_0, isotropic or average bonding parameter; K_o, coefficient of earth pressure at rest.

Fig. 11. Comparison between the settlement trough obtained using Peck's method and the multilaminate model.

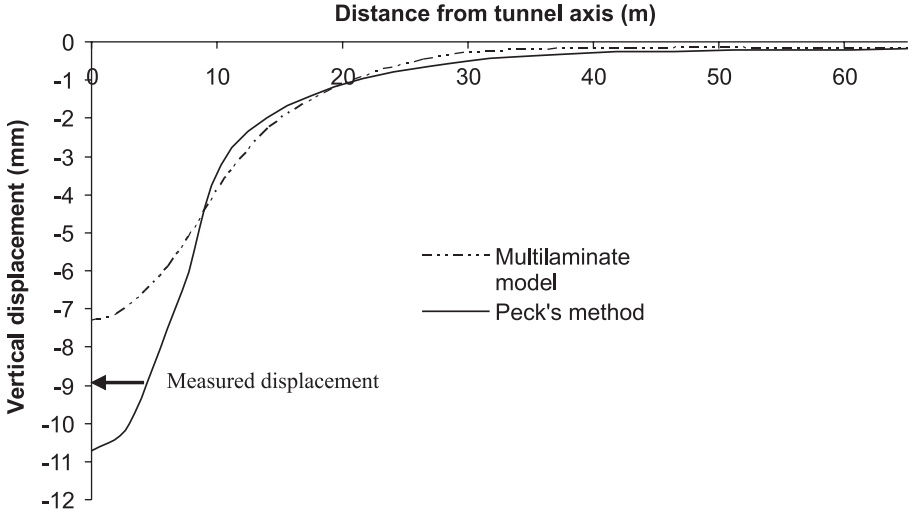

range of 0–2. Although the maximum displacement at the centreline of the tunnel slightly decreased as the bonding parameter increased, the width and the shape of the settlement trough was almost the same for the examined range of Ω_v values. The maximum settlement at the tunnel centreline decreased from 7.3 mm to about 6.7 mm as the anisotropy parameter increased from 0 to 2 as shown in Fig. 13. It was observed that if the soil bonding is ignored, depending on the value of Ω_v, the maximum settlement will be overestimated by up to 10%.

Fig. 12. Effect of anisotropy on the shape of the settlement trough.

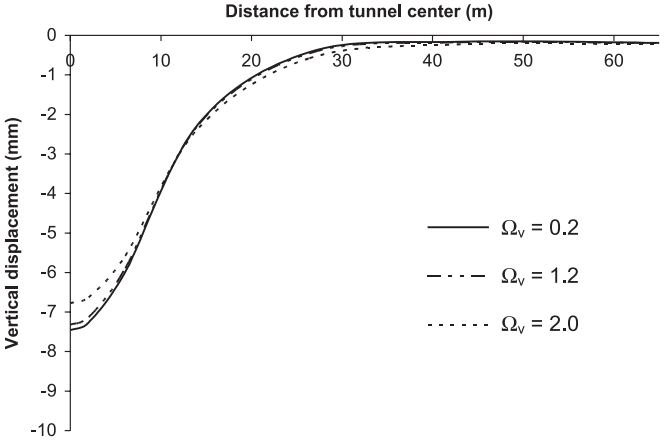

Fig. 13. Effect of anisotropy on the maximum surface displacement.

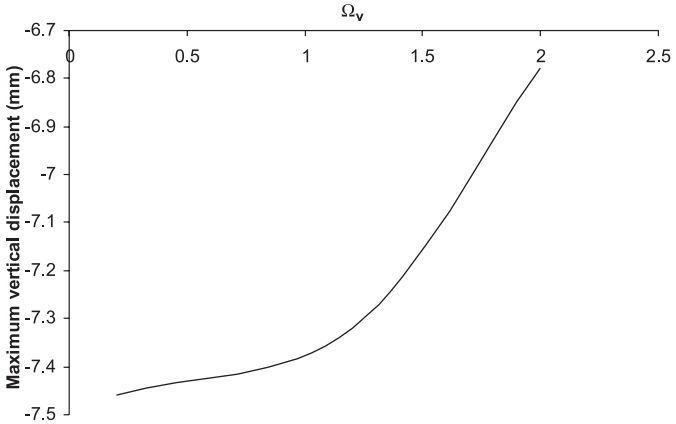

The effect of the anisotropy parameter, Ω_v, as well as the bonding parameter, b_0, on stresses developing in the concrete lining is investigated by varying the Ω_v value between 0.2 and 2 as shown in Fig. 14. The effect was found to be generally modest with a maximum stress difference at the tunnel crown where the stress decreased from 260 kPa to about 200 kPa as the value of Ω_v increased from 0.2 to 2.

The effect of anisotropy on the maximum surface settlement is examined in Fig. 15 for different OCR values. As OCR increased, displacement generally decreased. The rate of displacement reduction was found to depend on the anisotropy parameter as illustrated in Fig. 15, where the anisotropy parameter is plotted against the percentage change in stresses. Figure 16 shows the relationship between OCR and the ratio representing the differences in displacement calculated for the range of Ω_v between 0 and 2. It was observed that displacement increased almost linearly by up to 10% as the OCR increased from 1 to 2. A further increase in OCR was found to have an inverse effect on the surface settlement. For OCR = 5, no significant changes in the maximum surface displacements were observed for different Ω_v values.

Similarly, the effect of OCR on the changes in tangential and radial stresses for the range of Ω_v between 0 and 2 is examined in Figs. 17 and 18. Similar conclusions can be drawn from Fig. 17 where the change in tangential stresses increased almost linearly as OCR increased from 1 to 2 and obtained the peak value at OCR = 2, then the stresses decreased as the OCR increased beyond 2.

This observation has a significant implication on the assessment of the settlement induced by tunnelling for structured soils and the lining stresses for overconsolidated soils. If the soil bonding and the anisotropy are ignored, the settlement values may differ by up to 10%.

Effect of volume loss

The relationship between volume loss and the shape of the settlement trough tunnel is shown in Fig. 19. As the volume loss increased from 0% to 2.5%, the width of the settlement trough increased from 20 m to about 60 m. Another way of assessing the effects of volume loss on the maximum vertical displacement is shown in Fig. 20. An increase of about 7 mm was observed as the volume loss increased from 0% to 2.5%.

The effect of volume loss on lining stresses is examined in Fig. 21. The calculated lining stresses increased as the volume loss incrementally increased to 2.5%. Further volume loss was found to have no effect on the lining stresses. This may be attributed to the fact that at such high volume loss levels, the tunnel lining has already carried the full weight of the soil prism above the tunnel.

Effect of overconsolidation ratio (OCR)

The effect of OCR is investigated by considering an average OCR value for all the clay layers. The corresponding bonding parameter, b_0, is calculated using eq. [23] and the anisotropy parameter, Ω_v, is taken to be 1.2.

The effect of OCR on the shape of the settlement trough is shown in Figs. 22 and 23. It was found that the shape of the settlement trough is significantly influenced by a changing OCR. As the value of OCR increased from 1.2 to 5, the maximum vertical displacement increased from 4 to 10 mm. The width of the settlement trough also increased from about 25 m to more than 40 m for the investigated range of OCR values.

An increase in the lining stresses acting in the vertical direction (radial stresses at the crown and tangential stresses at the springline) was observed as the OCR value changed from 1 to 2. No further increase in vertical stresses was found for OCR values of more than 2 as shown in Fig. 24. However, lining stresses acting in the horizontal direction (tangential stresses at the crown and radial stresses at the springline) were found to continue increasing as the OCR value exceeded 2. This can be explained by the relationship between OCR and the coefficient of earth pressure at rest, K_o, (see eq. [24]) that controls the soil horizontal stress.

Effect of the yield locus shape and destructuration

Figure 25 shows the effect of the shape of the yield surface on the tunnelling induced lining stresses. The shape of the yield surface was found to have an insignificant effect on the lining stresses for the examined range of β. The effect of the destructuration parameter, a_r, on the surface settlement and the lining stresses was examined and reported elsewhere (Dang 2006). Negligible changes in surface movement and lining stresses were found. This was attributed to the fact that the tunnel was excavated in stiff clay at

Fig. 14. Effect of anisotropy on the lining stresses.

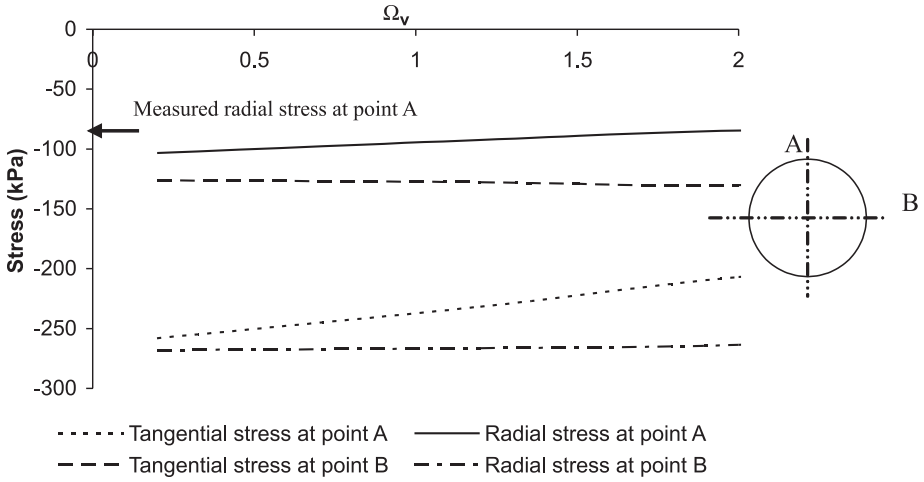

Fig. 15. Effects of anisotropy on the maximum surface displacement for different OCR values.

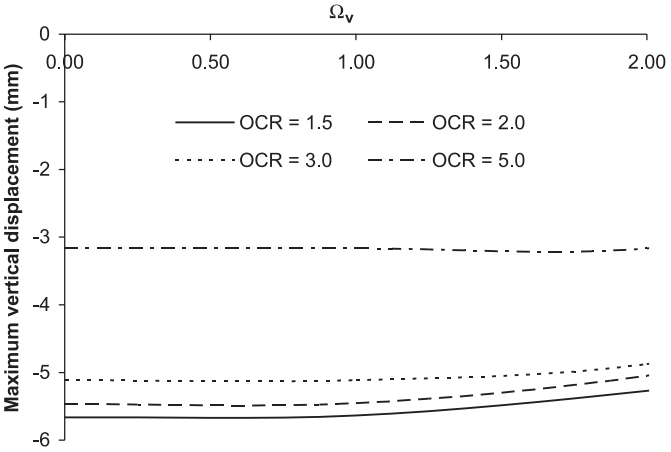

Fig. 16. Effect of OCR on the maximum surface displacement for Ω_v ranging between 0 and 2.

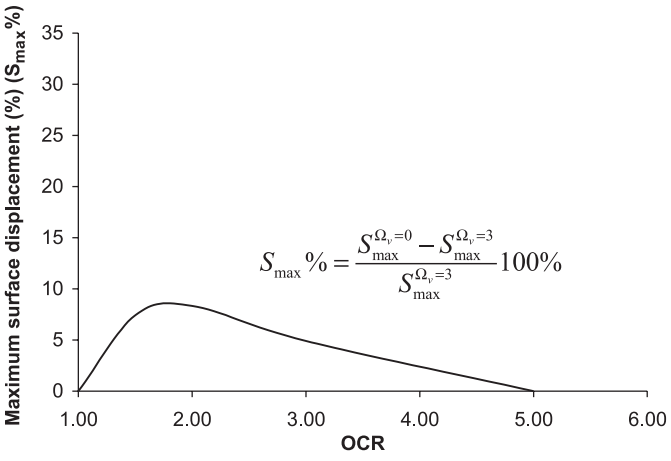

greater depth (17.5 m) below surface, and elastic response dominated the soil behaviour in the close vicinity of the tunnel. Further investigations of shallow tunnels in soft clays should be conducted to examine the effects of the above parameters on the ground response to tunnelling.

Fig. 17. Effect of OCR on the tangential stresses for Ω_v ranging between 0 and 2.

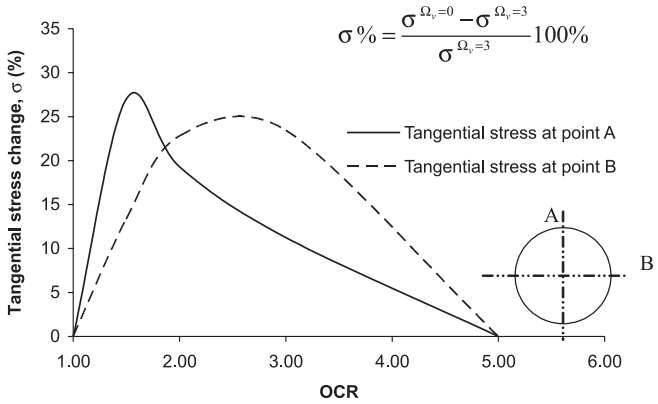

Summary and conclusions

The response of structured clays to shield tunnelling was numerically investigated in this study. A constitutive model that accounts for the effects of soil bonding, anisotropy, and destructuration was implemented into the Plaxis finite element software program. The model was used to simulate the construction of the Gatineau tunnel in Gatineau, Quebec. Calculated displacements and lining stresses were found to agree with the field measurements. The effects of volume loss, soil bonding, anisotropy, overconsolidation ratio, and shape of the yield surface were examined by conducting a parametric study to analyze the ground response and lining stresses to tunnel construction. The shape of the yield surface and the destructuration were found to have an insignificant effect on surface displacement and lining stresses. Soil bonding and anisotropy were found to have significant effects on surface settlement and lining stresses depending on the OCR value of the natural clay. As the OCR value increased from 1 to 2, the effect of bonding and anisotropy steadily increased. Further field verification of the above findings would be appropriate.

Fig. 18. Effect of OCR on the radial stresses for Ω_v ranging between 0 and 2.

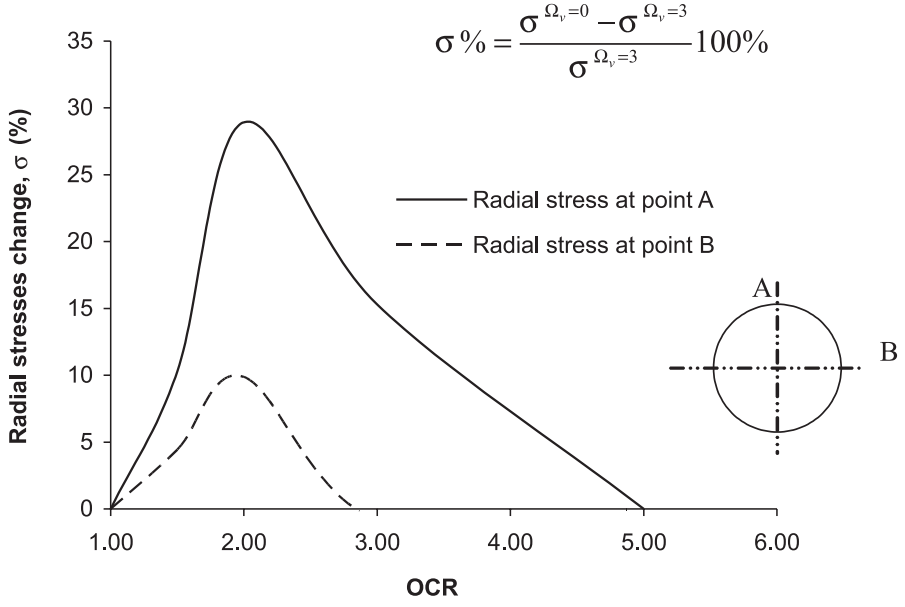

Fig. 19. Effect of volume loss on the settlement trough.

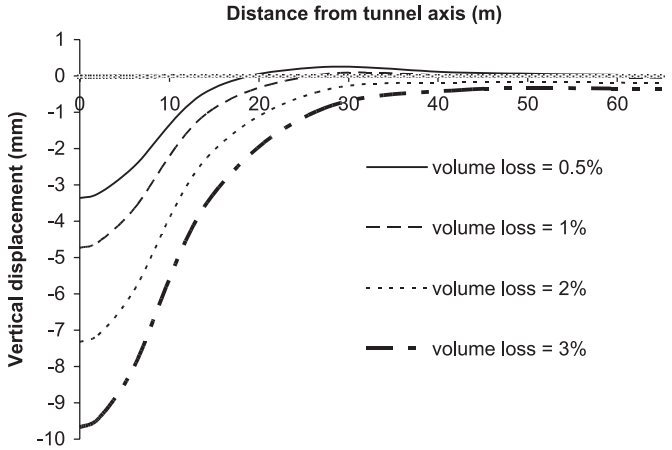

Fig. 20. Effect of volume loss on the maximum surface displacement.

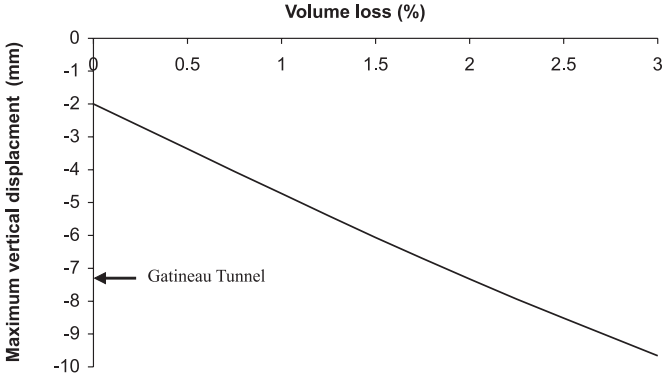

Fig. 21. Effect of volume loss on the lining stresses.

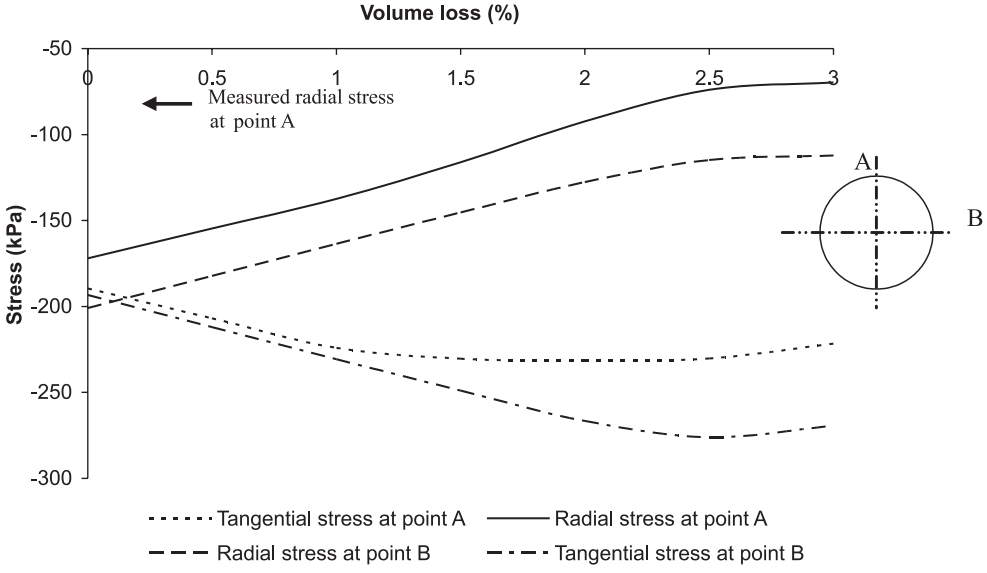

Fig. 22. Effect of OCR on the shape of the settlement trough.

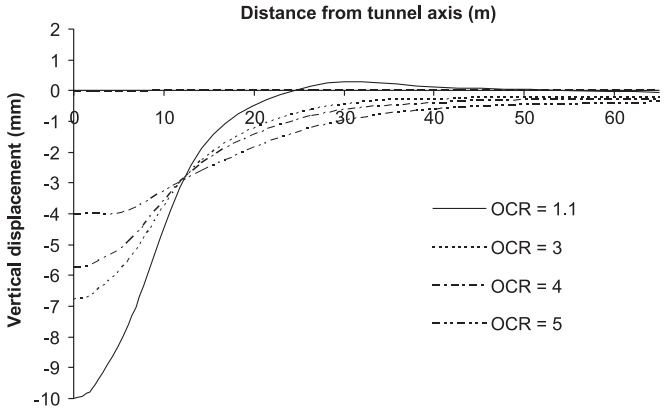

Fig. 23. Effect of OCR on the maximum surface displacement.

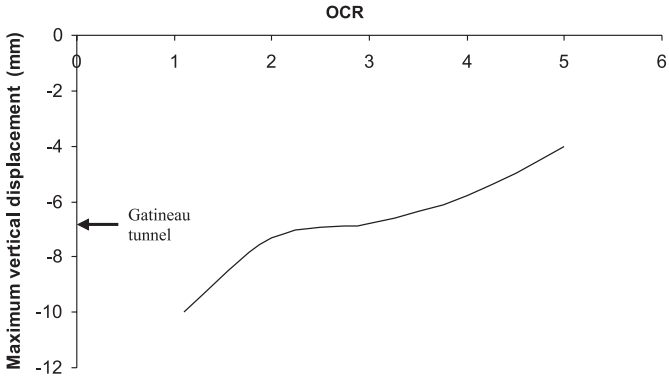

Fig. 24. Effect of OCR on the lining stresses.

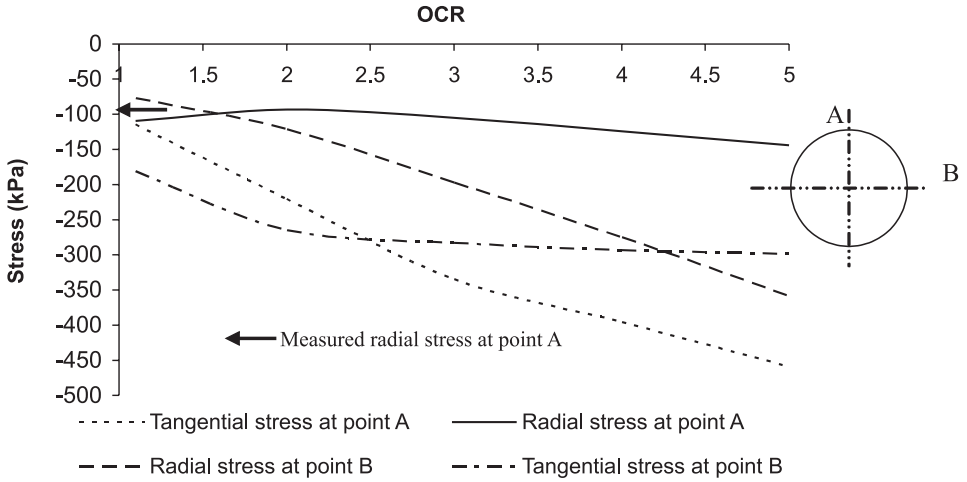

Fig. 25. Effect of the yield locus shape on lining stresses.

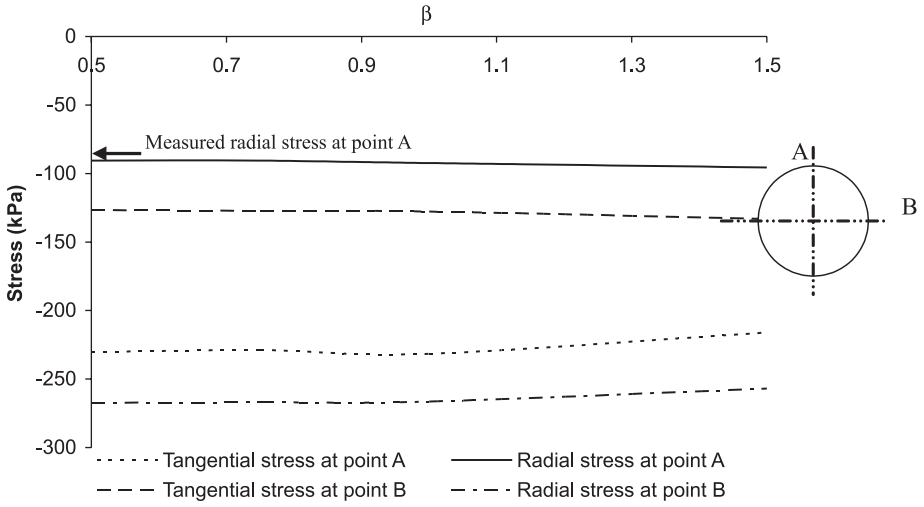

Acknowledgement

This research is supported by Fonds Québécois de la Recherche sur la Nature et les Technologies (FQRNT) and the Natural Sciences and Engineering Research Council of Canada (NSERC).

References

Addenbrooke, T.I., Potts, D.M., and Puzrin, A.M. 1997. Influence of pre-failure soil stiffness on the numerical analysis of tunnel construction. Géotechnique, **47**: 693–712.

Ballivy, G., Provencal, J., and Lefebvre, G. 1983. Étude du comportement d'une argile marine sensible (Champlain) a la periphérie d'un tunnel. *In* Proceedings of the 7th Panamerican Conference on Soil Mechanics and Foundation Engineering - PAN AM'83. Canadian Geotechnical Society, Vancouver, B.C. Vol. 1, pp. 343–354.

Calladine, C.R. 1971. A microstructural view of the mechanical properties of saturated clay. Géotechnique, **21**: 391–415.

Cudny, M., and Vermeer, P.A. 2004. On the modelling of anisotropy and destructuration of soft clays within the multi-laminate framework. Computers and Geotechnics, **31**: 1–22.

Dafalias, Y.F., Manzari, M.T., and Akaishi, M. 2002. A simple anisotropic clay plasticity model. Mechanics Research Communications, **29**: 241–245. doi:10.1016/S0093-6413(02)00252-5.

Dang, H.K. 2006. The application of a multilaminate model to simulate tunnelling in structured clays. M.Eng. thesis, Department of Civil Engineering and Applied Mechanics, McGill University, Montréal, Que.

Fliege, J., and Maier, U. 1996. A two-stage approach for computing cubature formulae for the sphere [online]. Ergebnisberichte Angewandte Mathematik, University Dormunt. Available from http://www.mathematik.uni-dortmund.de/Lsx/research/projects/fliege/nodes/nodes.html [accessed 4 September 2006].

Franzius, J.N., Potts, D.M., and Burland, J.B. 2005. The influence of soil anisotropy and K_o on ground surface movements resulting from tunnel excavation. Géotechnique, **55**: 189–199.

Gens, A., and Nova, R. 1993. Conceptual bases for a constitutive model for bonded soils and weak rock. *In* Geotechnical engineering of hard soils – soft rock. *Edited by* A. Anagnostopoulos, F. Schlosser, N. Kalteziotis, and R. Frank. A.A. Balkema, Rotterdam, Vol. 1, pp. 485–494.

Graham, J., and Houlsby, G.T. 1983. Anisotropic elasticity of a natural clay. Géotechnique, **43**: 165–180.

Karstunen, M., and Pande, G.N. 1997. Strain localization in granular media using multilaminate framework. *In* Applications of computational mechanics in geotechnical engineering. *Edited by* E.A. Vargas, R. F. Azevedo, and M. Matos.

Kumbhojkar, A.S., and Banerjee, P.K. 1993. An anisotropic hardening rule for saturated clays. International Journal of Plasticity, **9**: 861–888. doi:10.1016/0749-6419(93)90055-U.

Lee, K.M., and Rowe, R.K. 1990*a*. Finite element modelling of the three-dimensional ground deformations due to tunnelling in soft cohesive soils. Part I - method of analysis. Computers and Geotechnics, **10**: 87–109. doi:10.1016/0266-352X(90)90001-C.

Lee, K.M., and Rowe, R.K. 1990*b*. Finite element modelling of the three-dimensional ground deformations due to tunnelling in soft cohesive soils. Part II - results. Computers and Geotechnics, **10**: 111–138. doi:10.1016/0266-352X(90)90002-D.

Leroueil, S. 1992. A framework for the mechanical behaviour of structured soils, from soft clays to weak rocks. *In* Proceedings of the US–Brasil NSF Geotechnical Workshop on Applicability of Classical Coil Mechanics Principles to Structured Soils. *Edited by* A.S. Niet, Printec Press, Illinois, pp. 1–40.

Leroueil, S., Kabbaj, M., Tavenas, F., and Bouchard, R. 1985. Stress-strain-strain rate relation for the compressibility of sensitive natural clays. Géotechnique, **35**: 159–180.

Lo, K.Y., Ng, R.M., and Rowe, R.K. 1984. Predicting settlement due to tunnelling in clays. *In* Proceedings of Tunnelling in Soil and Rocks. Edited by K.Y. Lo, American Society of Civil Engineers, Vancouver, B.C. pp. 48–76.

Loganathan, N., and Poulos, H.G. 1998. Analytical prediction for tunnelling induced ground movements in clays. Journal of Geotechnical and Geoenvironmental Engineering, **124**: 846–856. doi:10.1061/(ASCE)1090-0241(1998)124:9(846).

Pande, G.N., and Sharma, K.G. 1983. Multi-laminate model of clays – A numerical evaluation of the influence of rotation of the principal stress axes. International Journal for Numerical and Analytical Methods in Geomechanics, **7**: 397–418. doi:10.1002/nag.1610070404.

Pande, G.N., and Yamada, M. 1994. The multilaminate framework of models for rock and soil masses. *In* Applications of computational mechanics in geotechnical engineering. *Edited by*R. Azevedo, E. Vargas, and L.M.R. Sousal, A.A. Balkema, Rotterdam, the Netherlands, pp. 105–123.

Park, K.H. 2004. Analytical solution for tunnelling-induced ground movement in clays. Tunnelling and Underground Space Technology, **20**: 249–261.

Peck, R.B. 1969. Deep excavations and tunneling in soft ground. *In* Proceedings of the 7th International Conference on Soil Mechanics and Foundation Engineering, Mexico City, State-of-the-Art Volume, pp. 225–290.

Plaxis. 2004. Plaxis finite element code for soil and rock analysis. Ver. 8. Plaxis PV. The Netherlands.

Potts, D.M., and Addenbrooke, T.I. 1997. Structure's influence on tunneling-induced ground movements. Proceedings of the Institution of Civil Engineers, Geotechnical Engineering, **125**(2): 109–125.

Pietruszczak, S., and Mroz, Z. 2000. On failure criteria for anisotropic cohesive-frictional materials. International Journal for Numerical and Analytical Methods in Geomechanics, **25**: 509–524.

Pietruszczak, S., and Pande, G.N. 1987. Multi-laminate framework of soil models – Plasticity formulation. International Journal for Numerical and Analytical Methods in Geomechanics, **11**: 651–658. doi:10.1002/nag.1610110610.

Pietruszczak, S., and Pande, G.N. 2001. Description of soil anisotropy based on multi-laminate framework. International Journal for Numerical and Analytical Methods in Geomechanics, **25**: 197–206. doi:10.1002/nag.125.

Rowe, R.K. 1983. Theoretical examination of the settlements induced by tunneling: four case histories. Canadian Geotechnical Journal, **20**: 299–314.

Sagaseta, C. 1987. Analysis of underained soil deformation due to ground loss. Géotechnique, **37**: 301–320.

Schuller, H., and Schweiger, H.F. 2002. Application of a multilaminate model to simulation of shear band information in NATM-tunnelling. Computers and Geotechnics, **29**: 501–524.

Su, S.F., Liao, H.J., and Lin, Y.H. 1998. Base stability of deep excavation in anisotropic soft clay. Journal of Geotechnical and Geoenvironmental Engineering, **124**: 809–819. doi:10.1061/(ASCE)1090-0241(1998)124:9(809).

Sun, D.A., Matsuoka, H., Yao, Y.P., and Ishii, H. 2004. An anisotropic hardening elastoplastic model for clays and sands and its application to FE analysis. Computers and Geotechnics, **31**: 37–46.

Van Baars, S. 2003. Soft soil creep modelling of large settlements. *In* Proceedings of the 2nd International Conference on Advances

in Soft Soil Engineering and Technology, Putrajaya, 2–4 July 2003. Edited by B.B.K. Huat. Kuala Lumpur, Malaysia, University Putra Malaysia Press, pp. 3–25.

Verruijt, A., and Booker, J.R. 1996. Surface settlement due to deformation of a tunnel in an elastic half space. Géotechnique, **46**: 753–756.

Wheeler, S.J., Cudny, M., Neher, H.P., and Wiltafsky, C. 2003. Some developments in constitutive modelling of soft clays. *In* Proceedings of the International Workshop on Geotechnics of Soft Soils - Theory and Practice, Noordwijkerhoud, the Netherlands, 17–19 September 2003. *Edited by* P.A. Vermeer, H.F. Schweiger, M. Karstunen, and M. Cudny, VGE Verlag Glückauf, Essen, pp. 3–22.

Wiltafsky, C., Messerklinger, S., and Schweiger, H.F. 2002. An advance multilaminate model for clay. Numerical models in geomechanics, NUMOG VIII, *Edited by* G.N. Pande and S. Pietrucszczak, Swets & Zeitlinger, Lisse, pp. 67–73.

Wood, D.M. 1990. Soil behaviour and critical state soil mechanics. Cambridge University Press, Cambridge.

Wood, D.M., and Graham, J. 1990. Anisotropic elasticity and yielding of a natural plastic clay. International Journal of Plasticity, **6**: 377–388. doi:10.1016/0749-6419(90)90009-4.